



HAL
open science

Anomalous birefringence of swollen lamellar phases : blue smectics

F. Nallet, Ph. Barois

► **To cite this version:**

F. Nallet, Ph. Barois. Anomalous birefringence of swollen lamellar phases : blue smectics. Journal de Physique II, 1994, 4 (6), pp.1049-1060. 10.1051/jp2:1994183 . jpa-00248013

HAL Id: jpa-00248013

<https://hal.science/jpa-00248013>

Submitted on 4 Feb 2008

HAL is a multi-disciplinary open access archive for the deposit and dissemination of scientific research documents, whether they are published or not. The documents may come from teaching and research institutions in France or abroad, or from public or private research centers.

L'archive ouverte pluridisciplinaire **HAL**, est destinée au dépôt et à la diffusion de documents scientifiques de niveau recherche, publiés ou non, émanant des établissements d'enseignement et de recherche français ou étrangers, des laboratoires publics ou privés.

Classification

Physics Abstracts

42.10Q — 61.30 — 82.70

Anomalous birefringence of swollen lamellar phases : blue smectics

F. Nallet and Ph. Barois

Centre de recherche Paul-Pascal, CNRS, Avenue A.-Schweitzer, 33600 Pessac, France

(Received 3 December 1993, received in final form 10 February 1994, accepted 18 February 1994)

Résumé. — La biréfringence d'une phase lamellaire lyotrope est calculée en fonction de la dilution. Nous montrons qu'elle peut s'annuler à condition que la biréfringence naturelle des bicouches de tensioactif soit positive. La dispersion au voisinage du point de biréfringence nulle est calculée. Ces résultats sont confirmés par des mesures de spectrophotométrie : la transmission des échantillons étudiés entre polariseurs croisés s'annule exactement pour une longueur d'onde particulière. La variation de l'intensité transmise en fonction de la longueur d'onde et de l'épaisseur des échantillons est conforme aux prévisions du modèle.

Abstract. — The birefringence of a lyotropic lamellar phase is calculated as a function of dilution. It is found to vanish and change sign, provided the natural birefringence of surfactant bilayers is positive. Dispersion is calculated about the point of zero birefringence. These predictions are illustrated with experiments of spectrophotometry : the intensity of light transmitted between crossed polarizers through several lamellar samples vanishes as expected at some particular wavelength. The dependence of the transmitted light on wavelength and cell thickness is consistent with theory.

1. Introduction.

It has been known for decades in chemical [1] and biological [2] systems that amphiphilic molecules can self-assemble to form supramolecular aggregates such as micelles, rods, lamellae or complex bidimensional periodic networks of non-intersecting surfaces.

The macroscopic appearance of such lyotropic phases is then related to the long-range organization of these aggregates : a disordered solution of micelles for instance can flow like a liquid whereas a cubic phase cannot. Liquid-crystalline structures (hexagonal, lamellar — i.e. smectic A — or nematic) are characterized by their optical birefringence.

In the particular case of lyotropic lamellar phases, the uniaxial symmetry is reflected by any second rank tensor that must be anisotropic with only two different eigenvalues. This structure for the dielectric tensor leads to an optical axis perpendicular to the average plane of the layers with a birefringence (i.e. extraordinary index n_e minus ordinary index n_o) usually positive [3].

Highly diluted lyotropic lamellar phases have recently received considerable theoretical [4-6] and experimental attention [7-9]. It has been observed in several cases that the birefringence exhibits a peculiar behaviour [10, 11] : for some particular value of the dilution, a non-oriented sample would appear uniformly dark and slightly coloured (actually blue in most of the reported experiments) whereas at higher and lower volume fractions of the solvent, the usual bright colours of a strongly birefringent material are observed. On the other hand, X-ray and neutron diffraction patterns [12] are perfectly regular when passing through this particular dilution (i.e. they show Bragg reflections at a wave vector $q_0 = 2\pi/d$, the layer spacing d increasing continuously upon dilution).

The aim of this paper is to show that this anomalous behaviour can be simply understood as the vanishing and the change of sign of the birefringence of the lamellar structure for a particular dilution. Such a change of sign of the birefringence had been reported long ago in aqueous solutions of AOT (sodium sulpho-di(2-ethylhexyl) succinic ester) [10]. We claim in the present paper that simple geometrical effects (so-called *form* birefringence) can explain this uncommon behaviour.

The birefringence of a regular stack of birefringent lamellae swollen by an isotropic solvent is calculated in the next section. It is found to vanish for some particular value of the layer spacing. The effect of the thermal fluctuations of the membranes is also considered. In section 3, the dispersion of the material is calculated about the wavelength for which the birefringence vanishes. Section 4 is then devoted to an experimental illustration of these results : the transmission of visible light through samples of different thicknesses between crossed polarizers is measured as a function of the wavelength.

2. Birefringence of a regular stack of lamellae in an isotropic solvent.

The form birefringence of a regular assembly of thin parallel plates of thickness e_1 and dielectric constant ε_1 in a continuous medium (solvent) of thickness e_2 and dielectric constant ε_2 has been known for a long time. In terms of refractive indices, it may be written as [13] :

$$n_e^2 - n_o^2 = - \frac{f_1 f_2 (n_1^2 - n_2^2)^2}{f_1 n_1^2 + f_2 n_2^2} \quad (2.1)$$

where $f_1 = e_1/(e_1 + e_2)$ and $f_2 = 1 - f_1$ are the volume fractions of the plates and of the solvent respectively and $n_i^2 = \varepsilon_i$, $i = 1, 2$.

Note that the assembly always behaves like a *negative* uniaxial crystal, regardless of the sign of the difference $n_1^2 - n_2^2$.

The birefringence of a real lyotropic lamellar phase is slightly more complex for two reasons : i) the *diluted* membrane is usually constituted of a sheet of parallel molecules of surfactant and therefore birefringent in itself and ii) thermal fluctuations of the membranes will affect their shape and therefore the birefringence of the structure. If the intrinsic birefringence of the membranes is positive, the birefringence of the lamellar structure is expected to be also positive at low solvent content but can become negative at high swelling if the form birefringence (2.1) prevails.

Indeed, at high swelling in the case of lamellar phases stabilized by entropic repulsion only [4], the membranes are crumpled [6-9] and their intrinsic birefringence falls off faster with dilution than the form birefringence of the stack. This is shown in the following, where the birefringence of the structure is calculated in a unit cell of thickness d and projected area A (from now on, d refers to the period of the lamellar stacking and e to the thickness of the membranes).

The electric \mathbf{E} and displacement \mathbf{D} fields in the solvent and in the membrane are respectively

$$\begin{aligned} D_{S_i} &= \epsilon_0 \epsilon_S E_{S_i} \\ D_{M_i} &= \epsilon_0 \epsilon_{M_{ij}} E_{M_j} \end{aligned} \tag{2.2}$$

where ϵ_S is the dielectric constant of the solvent (assumed to be an isotropic liquid) and $\epsilon_{M_{ij}}$ the dielectric tensor of the membrane (ϵ_0 is the permittivity of free space).

At this stage, it is convenient to define the local trihedron ($\mathbf{l}, \mathbf{m}, \mathbf{n}$) where \mathbf{n} and \mathbf{l}, \mathbf{m} are unit vectors perpendicular and tangent to the membrane respectively at position $\mathbf{r} = (x, y)$ (see Fig. 1). Primed and unprimed letters denote vector or tensor coordinates in this trihedron and in the macroscopic reference frame ($x, y, z = \text{optic axis}$) respectively.

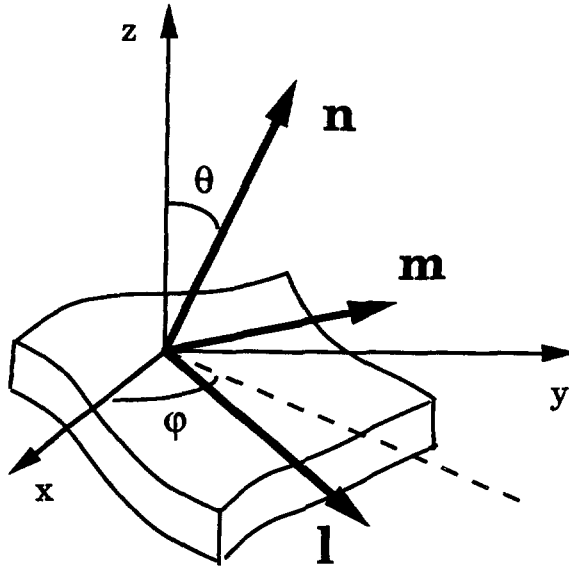


Fig. 1. — Definition of the local trihedron of unit vectors ($\mathbf{l}, \mathbf{m}, \mathbf{n}$) and of the angles ϕ and θ . The reference frame (x, y, z) is fixed and z is along the optical axis. The normal to the membrane at position \mathbf{r} is \mathbf{n} , and \mathbf{l} lies in the \mathbf{n} - z plane with its projection onto the x - y plane (dashed line) defining the angle ϕ .

The local relationship between the D_{S_i} and D_{M_i} is easy to express in ($\mathbf{l}, \mathbf{m}, \mathbf{n}$) since the normal component of the \mathbf{D} -field and the tangential component of the \mathbf{E} -field are continuous at the membrane-solvent interface

$$\begin{aligned} D'_{S3} &= D'_{M3} \Rightarrow \epsilon_S E'_{S3} = \epsilon'_{M33} E'_{M3} \\ E'_{S_i} &= E'_{M_i} \quad i = 1, 2. \end{aligned} \tag{2.3}$$

The effective macroscopic dielectric tensor ϵ^{eff} is defined as

$$\bar{D}_i = \epsilon_0 \epsilon_{ij}^{\text{eff}} \bar{E}_j \tag{2.4}$$

in which the bars denote spatial averages over the unit cell of volume $dx dy dz$

$$\bar{X}_i = \frac{1}{dA} \left[\int_{\text{solv}} d^3R X_{S_i} + \int_{\text{memb}} d^3R X_{M_i} \right] \tag{2.5}$$

with $X = D$ or E .

If $\theta(x, y)$ denotes the local angle between the normal $\mathbf{n}(x, y)$ and the optical axis z , the differential volume element of the membrane is $e \, dx \, dy / \cos \theta(x, y)$ with the assumption that the membrane thickness e (or equivalently the area per surfactant) keeps constant as the membranes fluctuate. The total volume of the membrane in the unit cell is then $eA \langle 1/\cos \theta \rangle$; the $\langle 1/\cos \theta \rangle$ term, first introduced by Helfrich and Servuss [14] has various consequences experimentally observed in lamellar, vesicles and sponge phase [15] which support the constant thickness assumption. The average values are then :

$$\bar{X}_i = X_{Si} \left(1 - \frac{e}{d} \left\langle \frac{1}{\cos \theta} \right\rangle \right) + \frac{e}{d} \left\langle \frac{X_{Mi}}{\cos \theta} \right\rangle \tag{2.6}$$

$X = D$ or E , $i = 1, 2, 3$ and the brackets $\langle \cdot \rangle$ denote thermal averages over wavevectors larger than those of visible light.

Inserting the three relations (2.3) expressed in the (x, y, z) frame into the six equations (2.6) will lead to the form (2.4). \bar{D} for example can be calculated as :

$$\bar{D}_i = \epsilon_0 \left[\epsilon_S \left(1 - \frac{e}{d} \left\langle \frac{1}{\cos \theta} \right\rangle \right) E_{Si} + \frac{e}{d} A_{ik} E_{Sk} \right] \tag{2.7}$$

with

$$A_{ik} = \left\langle \frac{M_{ij} \epsilon'_{j\ell} (M^{-1})_{\ell k}}{\cos \theta} \right\rangle$$

and

$$\epsilon'_{j\ell} = \begin{bmatrix} \epsilon_{M\perp} & 0 & 0 \\ 0 & \epsilon_{M\perp} & 0 \\ 0 & 0 & \epsilon_S \end{bmatrix}.$$

The matrix $M_{ij}(\theta, \varphi)$ changes coordinates from the (x, y, z) set of axes (unprimed) to the $(\mathbf{l}, \mathbf{m}, \mathbf{n})$ trihedron (primed) : $X_i = M_{ij} X'_j$. The matrix A_{ij} is diagonal as expected after trivial angular averaging over the azimuthal angle φ .

Calculating \bar{E} likewise and eliminating the E_{Si} 's leads to the final result for small θ :

$$\epsilon_{\perp}^{\text{eff}} = n_o^2 = \epsilon_S \frac{1 + \frac{e}{d} \left(\frac{\epsilon_{M\perp} - \epsilon_S}{\epsilon_S} \right)}{1 + \frac{e}{d} \left(\frac{\epsilon_S - \epsilon_{M\parallel}}{2 \epsilon_{M\parallel}} \right) \langle \theta^2 \rangle} \tag{2.8a}$$

$$\epsilon_{\parallel}^{\text{eff}} = n_e^2 = \epsilon_S \frac{1 + \frac{e}{d} \left(\frac{\epsilon_{M\perp} - \epsilon_S}{\epsilon_S} \right) \langle \theta^2 \rangle}{1 + \frac{e}{d} \left(\frac{\epsilon_S - \epsilon_{M\parallel}}{\epsilon_{M\parallel}} \right) \left(1 - \frac{\langle \theta^2 \rangle}{2} \right)}. \tag{2.8b}$$

At lowest (zeroth) order in θ^2 , the birefringence is therefore controlled by :

$$n_e^2 - n_o^2 = \left(\frac{e}{d} \right) \frac{(\epsilon_S - \epsilon_{M\parallel})(\epsilon_{M\perp} - \epsilon_S)(1 - e/d) + \epsilon_S(\epsilon_{M\parallel} - \epsilon_{M\perp})}{\epsilon_{M\parallel} + (e/d)(\epsilon_S - \epsilon_{M\parallel})} \tag{2.9}$$

It vanishes for :

$$1 - \frac{e}{d} = \frac{\epsilon_S(\epsilon_{M\perp} - \epsilon_{M\parallel})}{(\epsilon_S - \epsilon_{M\parallel})(\epsilon_{M\perp} - \epsilon_S)}. \tag{2.10}$$

As $(1 - e/d)$ is always positive, the condition (2.10) can be fulfilled in two cases only :
 i) positive birefringence of the membrane ($\epsilon_{M\parallel} > \epsilon_{M\perp}$) and : $\epsilon_S > \epsilon_{M\parallel}$ or $\epsilon_S < \epsilon_{M\perp}$;
 ii) negative birefringence of the membrane and $\epsilon_{M\parallel} < \epsilon_S < \epsilon_{M\perp}$.

Films of surfactant usually exhibit a positive birefringence. Case i) is therefore the more likely observed.

Thermal averages of angular fluctuations of the membranes $\langle \theta^2 \rangle$ over wavevectors larger than those of visible light obviously depend on the systems : lamellar phases stabilized by electrostatic interactions will fluctuate much less than sterically stabilized systems. $n_c^2 - n_o^2$ is plotted as a function of the lattice period d in figure 2 for a set of flat rigid membranes (2.9) and undulating flexible membranes (2.8). In both cases, the birefringence is positive at small lattice period d , it falls off with dilution, passes through zero to reach a negative minimum and vanishes again asymptotically as $-1/d$.

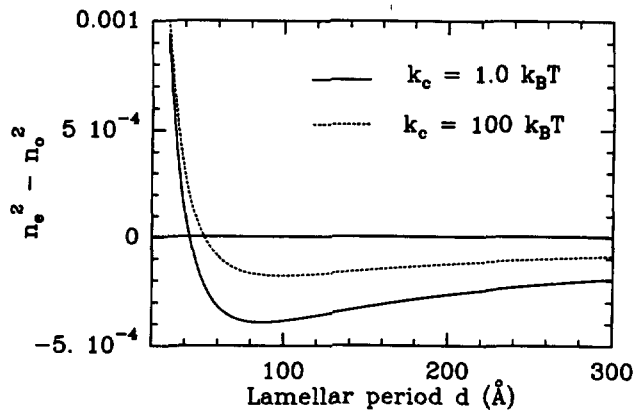


Fig. 2. — Plot of the dielectric anisotropy $n_c^2 - n_o^2$ against the period of the lamellar phase. The relative permittivities are $\epsilon_S = 2.02$ for the solvent (e.g. dodecane), $\epsilon_{M\parallel} = 1.83$ and $\epsilon_{M\perp} = 1.82$ for the membrane of thickness 20 Å. The two curves correspond to different membrane bending moduli k_c : $-1 - k_c = 100 k_B T$ (rigid membrane), dashed line and $-2 - k_c = 1.0 k_B T$ (flexible membrane), solid line. Thermal fluctuations of the flexible membrane are calculated assuming that the lamellar phase is stabilized by steric repulsion only, which yields : $\langle \theta^2 \rangle = (2 \pi)^{-1} k_B T/k_c \ln (d/a)$ [16].

The vanishing of the birefringence is thus expected when the negative contribution of the dilution (i.e. form birefringence) compensates exactly the positive birefringence of the membranes. Figure 2 shows that this condition should be met in typical lyotropic systems.

The dielectric permittivities ϵ_S , $\epsilon_{M\parallel}$ and $\epsilon_{M\perp}$ however depend on the frequency of the electromagnetic wave within the optical range so that for a particular dilution e/d equation (2.10) is satisfied for a single pulsation ω_0 only. The optical behaviour of such a lamellar phase about this particular value ω_0 will be calculated in the next section.

3. Dispersion about the dilution of zero birefringence.

We now consider a macroscopic uniaxial lamellar phase. The vector field \mathbf{n} denotes the optical axis, perpendicular to the average plane of the layers. The (frequency dependent) dielectric tensor ϵ_{ij} reads

$$\epsilon_{ij} = \bar{\epsilon} \delta_{ij} + \Delta \epsilon \left(n_i n_j - \frac{1}{3} \delta_{ij} \right). \tag{3.1}$$

The ordinary and extraordinary indices of refraction are given by $n_o^2 = \bar{\epsilon} - 1/3 \Delta\epsilon$ and $n_e^2 = \bar{\epsilon} + 2/3 \Delta\epsilon$ respectively.

As argued in the previous section, the optical anisotropy $\Delta\epsilon$ depends on the dilution of the lamellar phase and may vanish at some frequency ω_0 in the visible range. Since we want to describe the optical properties of the lamellar phase in the vicinity of ω_0 , we shall consider a lowest order expansion of $\Delta\epsilon$

$$\Delta\epsilon = \delta\epsilon_1 \left(\frac{\omega - \omega_0}{\omega_0} \right). \quad (3.2)$$

We will see that this dispersion gives to the weakly-birefringent « blue smectic » its peculiar anisotropic optical properties in the vicinity of ω_0 .

In a coordinate system defined as follows : $n_i = \delta_{i3}$, $\mathbf{k} = k(\sin \theta, 0, \cos \theta)$, the two propagative modes read :

i) *ordinary wave* :

$$k_o^2 = \frac{\omega^2}{c^2} n_o^2 \quad (3.3a)$$

and polarization such that \mathbf{D} is perpendicular to both \mathbf{k} and \mathbf{n} ;

ii) *extraordinary wave* :

$$k_e^2 = \frac{\omega^2}{c^2} \frac{n_o^2 n_e^2}{n_o^2 \sin^2 \theta + n_e^2 \cos^2 \theta} \quad (3.3b)$$

and polarization such that \mathbf{D} is perpendicular to \mathbf{k} , in the (\mathbf{k}, \mathbf{n}) -plane.

If a well aligned sample of such a lamellar material of thickness D is sandwiched between crossed polarizers, the intensity of the transmitted light can be calculated as a function of frequency ω (or wavelength *in vacuo* λ) and direction θ — referred to optical axis — of the incident light as [13] :

$$\frac{I(\omega, \theta, \alpha)}{I_0} = \sin^2 2\alpha \sin^2 \left[\frac{D}{2} (k_e - k_o) \right] \quad (3.4)$$

in which I_0 is the intensity of the incident light linearly polarized along direction x and α is the angle between this direction of polarization and the projection of the optical axis on a wave plane (Fig. 3).

The transmitted intensity I/I_0 is calculated and plotted against wavelength λ for a well aligned sample with optical axis oriented perpendicularly to the direction of propagation — i.e. $\theta = \pi/2$ — (Fig. 4a) and for a randomly oriented sample — i.e. a powder in the crystallographic sense — (Fig. 4b). The parameters we have chosen in this illustration are : $\bar{\epsilon} = 2$, independent of frequency ; $\Delta\epsilon(\omega) = 10^{-4}(\omega - \omega_0)/\omega_0$ and wavelength $\lambda_0 = 510$ nm. Three thicknesses $D = 5, 20$ and 40 nm are represented. The relative transmitted intensity I/I_0 is zero at wavelength λ_0 for both well aligned and randomly oriented samples. It oscillates on both sides of λ_0 at a scale that depends on the optical path D . The period is actually proportional to $1/D$ for the aligned crystal whereas powder averaging strongly decreases the amplitudes and slightly shifts the extrema of the secondary oscillations. In the experimentally common case of a randomly oriented sample we note that most of the transmitted light has a shorter wavelength than λ_0 . The sample would then appear as blue in the example of figure 4b. However, the characteristic wavelength λ_0 for which the birefringence goes to zero depends on

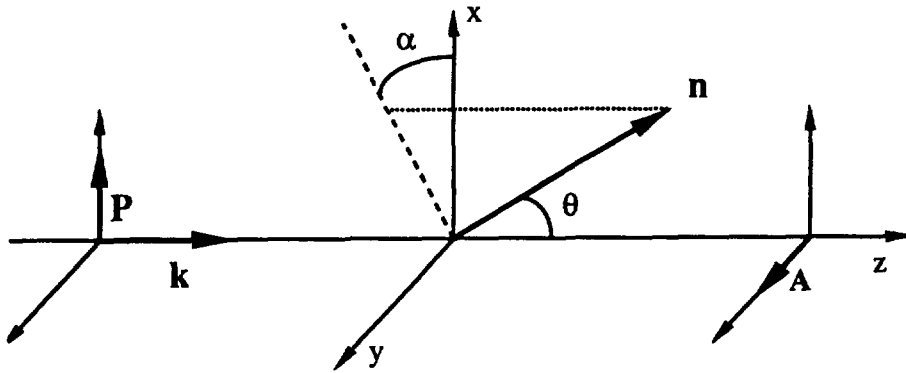


Fig. 3. — Schematic drawing of the light transmission experiment. The wave vector k of the propagating light is along axis z . The polarization P of the incident light is along axis x , with a crossed analyzer A along axis y . The orientation of the optical axis n of the birefringent material is described in spherical coordinates by co-latitude θ and azimuth α .

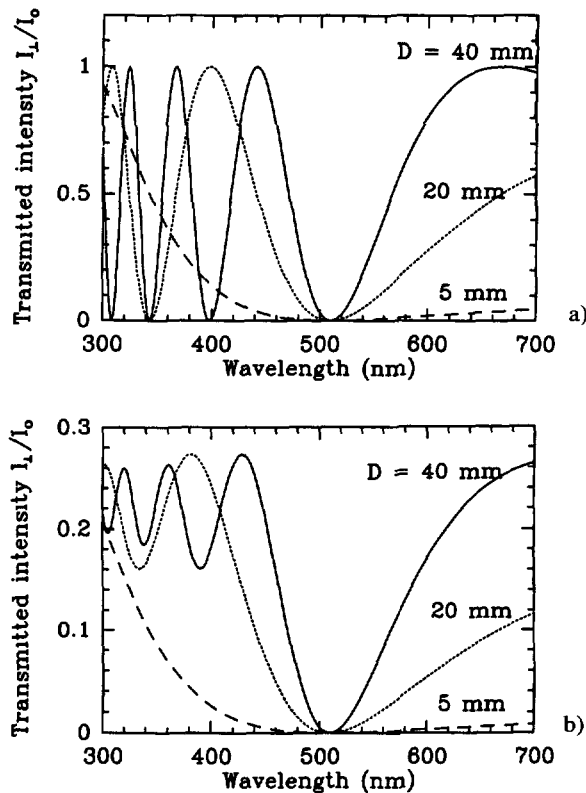


Fig. 4. — Relative transmitted intensity between crossed polarizers, calculated from relations (3.3) and (3.4), as a function of the wavelength *in vacuo* of the incident light. Figure 4a corresponds to an oriented material, with optical axis perpendicular to the propagation direction ($\theta = \pi/2$) and $\alpha = \pi/4$, while figure 4b is relevant for a powder sample. Three different optical paths D have been considered. The wavelength at which the birefringence is zero is $\lambda_0 = 510$ nm (for other parameters, see text); note that zero transmission occurs at wavelength λ_0 , whatever the optical path.

the layer spacing as shown in section 2 : the transmitted colour thus varies with the weight fraction of surfactant. This point is consistent with experimental observations (see next part).

At frequency ω_0 , it would appear from the constitutive equation (2.4) that the *uniaxial* medium is optically *isotropic*. This is not quite true, because equation (2.4) is actually the lowest order term of an expansion in spatial derivatives of the electric field. The general relation between the electric field \mathbf{E} and the dielectric displacement \mathbf{D} should read

$$D_i = \varepsilon_0 [\varepsilon_{ij} E_j + \mu_{ijkl} \partial_{kl}^2 E_j + \dots] \quad (3.5)$$

in which μ_{ijkl} is a phenomenological tensor of rank 4 with uniaxial symmetries. There are no first-order derivatives of the field in this expression, since their presence is ruled out by the inversion symmetry of the systems we consider. Of course, such terms have to be written when there is no inversion symmetry : they are responsible for the optical activity of isotropic solutions of chiral compounds, for instance [13].

The second-order derivatives generate a tensor contribution of rank 2 $\mu_{ijkl} k_k k_l$ in which the wavevector components $k_k k_l$ kill the uniaxial symmetry. It follows that the cancellation of the birefringence may not occur at all incidences θ . As a result, the powder sample should transmit a weak intensity (of order μ) between crossed polarizers at frequency ω_0 . We shall see in the next section that this effect is not detected experimentally which confirms that the μ_{ijkl} 's contribution is negligible.

At last, one should note that we used in figure 4 the simple first-order expansion of $\Delta\varepsilon$ (3.2) all over the frequency range of visible light. For frequencies ω significantly different from ω_0 higher order terms in $(\omega - \omega_0)/\omega_0$ are expected to become important. Figures 4a and 4b must therefore be considered as accurate close to ω_0 and only qualitatively correct elsewhere.

4. Experimental section.

An anomalous birefringence of lamellar phases similar to that described in the previous sections has been reported in several lyotropic systems [10, 11]. In order to check the relevance of our description, we have chosen to investigate the quaternary system Sodium Dodecyl Sulfate (SDS), hexanol, dodecane and water. This system forms a lamellar phase over a wide range of oil concentrations (see Fig. 5 for a pseudo-ternary phase diagram).

Samples prepared along the dotted line of figure 5 exhibit a dark unique colour between crossed polarizers (from blue to yellow depending on the composition). This feature shows an anomaly of the birefringence whereas neutron diffraction patterns show no singular behaviour of the layered structure [12b].

Four different compositions were prepared with the same weight fraction of hexanol ($x_H = 16\%$) and constant water/surfactant ratio ($x_W/x_S = 4.3$). They are labelled relative to their dodecane weight fraction x_D . S45 ($x_D = 45.0\%$), S48, S51 and S54. After preparation, the mixtures were left several days at room temperature (20 °C) until they look clear and homogeneous. All the samples showed coloured patches separated by darker regions between crossed polarizers. The observed colour was obviously characteristic of the composition.

The photometric measurements were carried out in the visible range (300-700 nm) with a Perkin-Elmer Model 330 spectrophotometer. The samples were introduced in amorphous quartz cells with optical paths of 5, 10, 20 and 40 mm. Two identical cells were prepared in each case to balance the two ways of the spectrophotometer : one was put between crossed polarizers in the main beam (transmitted intensity I_\perp) whereas the other one was mounted between parallel polarizers in the reference beam (transmitted intensity I_\parallel). The recorded signal I_\perp/I_\parallel was therefore insensitive to the wavelength-dependent absorption of the polarizers, the cells and the samples.

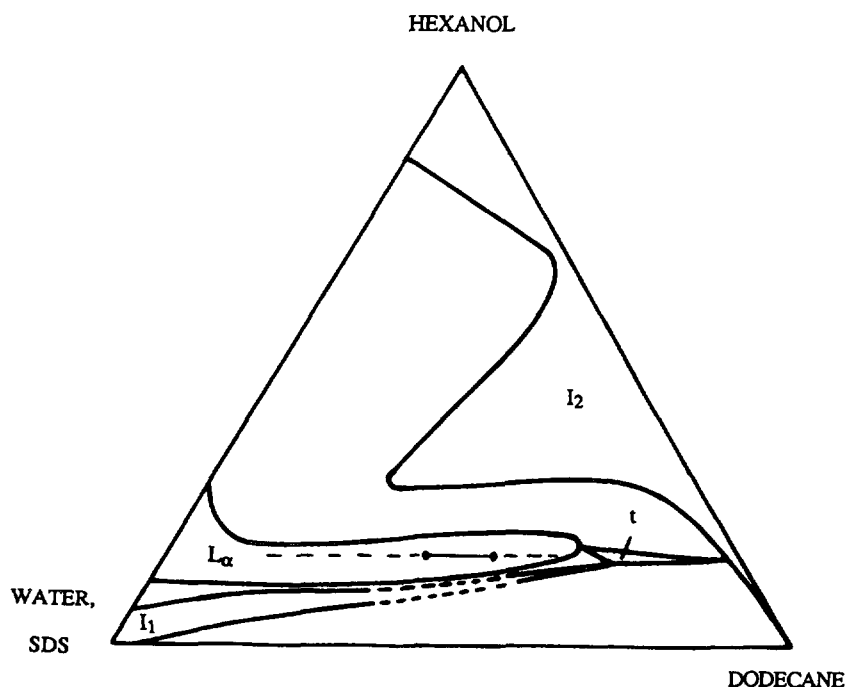


Fig. 5. — Pseudo-ternary phase diagram at temperature $T = 21^\circ\text{C}$ of the SDS/hexanol/water/dodecane system, taken from reference [11] (see also Ref. [17]). The water over surfactant mass ratio x_w/x_s is 4.3. The line shows the dilution path followed in the lamellar L_α phase in our experiment. I_1 and I_2 are respectively direct and inverse micellar phases. t is an $I_1 - I_2 - L_\alpha$ three phase equilibrium.

A typical series of spectra for different thicknesses is reported in figure 6 (sample S51). The ratio I_\perp/I_\parallel is zero (i.e. less than 4×10^{-4}) for a particular wavelength $\lambda_0 = 393 \pm 5$ nm. Oscillations on either sides of this fixed point λ_0 are then observed at a scale that gets shorter upon increasing the thickness of the cells.

The theoretical value of the measured ratio I_\perp/I_\parallel is easily obtained from equation (3.4) :

$$\left(\frac{I_\perp}{I_\parallel}\right)_{\text{theor}} = \frac{I(\omega, \theta, \alpha)/I_0}{1 - I(\omega, \theta, \alpha)/I_0} \quad (4.1)$$

Equation (4.1) applies for a single crystal. Angular averaging over α and θ with appropriate distribution function has to be performed for our non-oriented samples.

The theoretical ratio I_\perp/I_\parallel is plotted in figure 7 in the case of a randomly oriented sample. It vanishes at wavelength λ_0 and oscillates on both sides with a finite amplitude : the maxima and secondary minima are non-zero and lower than 1. In the case of a well oriented sample (not plotted), the behaviour is qualitatively the same but with different amplitudes : the ratio $I(\omega, \theta = \pi/2, \alpha)/I_0$ oscillates between zero and $\sin^2 2\alpha$ which in turn implies that I_\perp/I_\parallel oscillates between zero and $\tan^2 2\alpha$ i.e. with unbound amplitude.

In our experiments, the situation is obviously intermediate : our samples are neither oriented nor perfectly isotropic since the colouring between crossed polarizers is not uniform. Indeed, the amplitude of the oscillations on either sides of λ_0 can change significantly upon ageing or gentle shaking. We have not tried to fit the experimental curves since their actual shapes depend too much on an unknown angular distribution function of the crystallites.

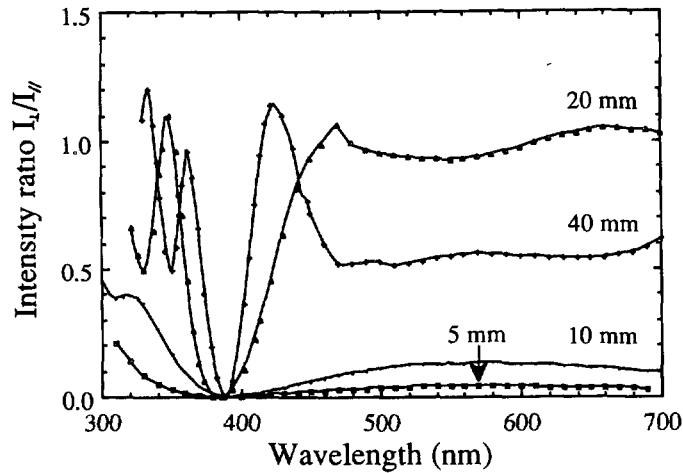


Fig. 6. — Transmitted intensity between crossed polarizers (I_{\perp}) relative to the one between parallel polarizers (I_{\parallel}), for a particular sample — S51 — along the dilution line, as a function of the wavelength *in vacuo* of the incident light. The optical path ranges from 5 mm to 40 mm. The wavelength of zero transmission is about 393 nm, independent of the optical path.

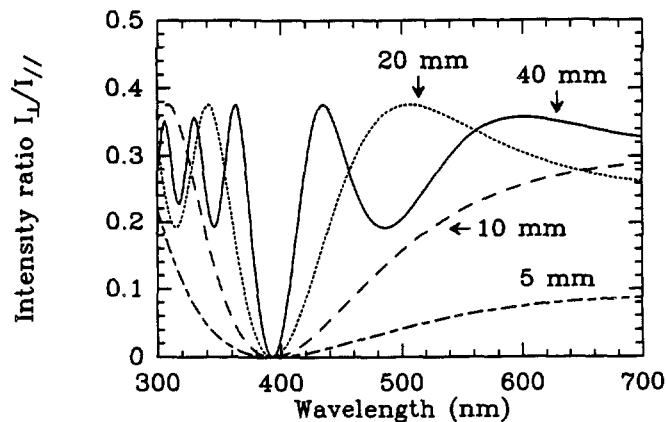


Fig. 7. — Theoretical variation of the ratio of the transmitted intensities I_{\perp} (crossed polarizers) to I_{\parallel} (parallel polarizers) in the case of a randomly oriented sample. The wavelength of zero transmission is set to 393 nm to match the experimental value (see Fig. 6) and the same four optical paths D are represented. Other parameters are $\epsilon = 2.0$ and $\Delta\epsilon = 2 \times 10^{-4}(\omega - \omega_0)/\omega_0$. The experimental behaviour is qualitatively well reproduced. The amplitude of the secondary oscillations is found to increase when the distribution of orientation of the optical axis changes from isotropic to partially oriented, which is consistent with experimental observations (see text and Fig. 6).

The experimental behaviour is however very similar to the calculated ratio I_{\perp}/I_{\parallel} (Fig. 7). All samples exhibit a zero birefringence for a particular wavelength λ_0 which depends on composition (see Tab.) but not on the thickness of the sample (Fig. 6). Secondary oscillations are observed in all samples with a period that decreases upon increasing thickness. The value of the secondary minima is non-zero and changes slowly upon ageing. We interpret this observation as a slow variation of the distributions of angles α and θ with time.

Table I. — Wavelengths λ_0 for which the transmission between crossed polarizers vanishes exactly, given for four different samples along a line with constant hexanol weight content ($x_A = 0.16$) and constant water over surfactant ratio ($x_W/x_S = 4.3$). Each sample was tested in four cells with different thicknesses (5, 10, 20 and 40 nm). Variations in λ_0 with thickness were less than 5 nm (1.5 %).

Sample	Weight fractions (%) SDS/hex./water/dodecane	Wavelength of zero birefringence (nm)
S45	7.4/16.0/31.6/45.0	320
S48	6.8/16.0/29.2/48.0	350
S51	6.2/16.0/26.8/51.0	393
S54	5.7/16.0/24.4/54.0	477

At last, we note that the first-order approximation of $\Delta\varepsilon$ in powers of $(\omega - \omega_0)/\omega_0$ (3.2) reproduces remarkably well the experimental behaviour : higher order terms do not seem to contribute very much in the visible range. This does not mean however that the experiments are not sensitive to the real variations of $\Delta\varepsilon$ with frequency. In terms of wavelength, (3.2) reads

$$\Delta\varepsilon = \delta\varepsilon_1 \left(\frac{\lambda_0 - \lambda}{\lambda} \right) \quad (4.2)$$

which implies that $\Delta\varepsilon$ varies relatively quicker with λ below λ_0 than above. This is actually the case in our experiments : the period of the oscillations of the transmitted light is clearly shorter below λ_0 .

5. Conclusion.

We have shown in this paper that the anomalous birefringence of diluted lyotropic smectics can be simply understood as the vanishing of the birefringence at some particular dilution for which the negative form birefringence of the stack of lamellae matches exactly the positive birefringence of each lamella. Exact cancellation only occurs at a particular wavelength λ_0 which depends on composition. Samples illuminated with white light between crossed polarizers transmit all wavelength but λ_0 and thus exhibit uniform pastel colours.

Measurements of transmitted intensities between crossed polarizers are consistent with theoretical expectations and hence support the model.

Close to λ_0 , the birefringence and subsequently anisotropic optical properties are very sensitive to thermal undulations of the membranes (see formulae (2.8)). This phenomenon could be used to probe the effect of temperature or external fields on these fluctuations for instance.

Acknowledgments.

We wish to thank D. Roux and G. Porte for helpful discussions.

References

- [1] Ekwall P., Advances in Liquid Crystals, G. H. Brown Ed. (Academic Press, New York, 1975).
- [2] Bouligand Y., *J. Phys. Colloq France* **51** (1990) C7-35.
- [3] Kelker H. and Hatz R., Handbook of Liquid Crystals (Verlag Chemie, Weinheim, Deerfield, 1980).

- [4] Helfrich W., *Z. Naturforsch.* **33a** (1978) 305.
- [5] Leibler S. and Lipowski R., *Phys. Rev. B* **35** (1987) 7004.
- [6] Golubovic L. and Lubensky T. C., *Phys. Rev. B* **39** (1989) 12110.
- [7] DiMeglio J.-M., Dvolaitzky M., Léger L. and Taupin C., *Phys. Rev. Lett.* **54** (1985) 1686.
- [8] Larché F. C., Appell J., Porte G., Bassereau P. and Marignan J., *Phys. Rev. Lett.* **56** (1986) 1700.
- [9] Safinya C. R., Roux D., Smith G. S., Sinha S. K., Dimon P., Clark N. A. and Bellocq A.-M., *Phys. Rev. Lett.* **57** (1986) 2718.
- [10] Rogers J. and Winsor P. A., *Nature* **216** (1967) 477.
- [11] Roux D., thèse d'Etat, Université Bordeaux-I, n 810 (1984).
- [12] a) Nallet F., Laversanne R. and Roux D., *J. Phys. II France* **3** (1993) 487 ;
b) Roux D. and Nallet F., unpublished neutron scattering work on the quaternary system investigated in the present paper.
- [13] Born M. and Wolf E., *Principles of Optics* (Pergamon Press, Oxford, 1975).
- [14] Helfrich W. and Servuss R. M., *Nuovo Cimento* **3** (1984) 137.
- [15] See for instance Strey R., Schomäcker R., Roux D., Nallet F. and Olsson U., *J. Chem. Soc. Faraday Trans.* **86** (1990) 2253 ;
Skouri M., Marignan J., Appell J. and Porte G., *J. Phys. II France* **1** (1991) 1121.
- [16] de Gennes P.-G. and Taupin C., *J. Phys. Chem* **86** (1982) 2294.
- [17] Roux D. and Bellocq A.-M., *Physics of Amphiphiles : Micelles, Vesicles and Microemulsions*, V. Degiorgio and M. Corti Eds. (North-Holland Physics Publishing, Amsterdam, 1985) ;
Bellocq A.-M., *Physics of Complex and Supermolecular Fluids*, S. A. Safran and N. A. Clark Eds. (John Wiley & Sons, New York, 1987).